Received 9 September 2019; revised 24 October 2019; accepted 30 October 2019. Date of publication 9 September 2019;
date of current version 18 November 2019. The review of this article was arranged by Editor A. G. U. Perera.

Digital Object Identifier 10.1109/JEDS.2019.2951203

Effective Evaluation Strategy Toward Low Temperature Solution-Processed Oxide Dielectrics for TFT Device

WEI CAI[1], HONGLONG NING[1], SHANGXIONG ZHOU[1], ZHENNAN ZHU[1], RIHUI YAO[1], JIANQIU CHEN[1], RUIQIANG TAO[2,3], ZHIQIANG FANG[4], XUBING LU[2], AND JUNBIAO PENG[1]

1 Institute of Polymer Optoelectronic Materials and Devices, State Key Laboratory of Luminescent Materials and Devices, South China University of Technology, Guangzhou 510640, China
2 Institute for Advanced Materials, South China Normal University, Guangzhou 510006, China
3 Guangdong Provincial Key Laboratory of Quantum Engineering and Quantum Materials, South China Normal University, Guangzhou 510006, China
4 State Key Laboratory of Pulp and Paper Engineering, South China University of Technology, Guangzhou 510640, China

CORRESPONDING AUTHORS: H. NING and R. YAO (e-mail: ninghl@scut.edu.cn; yaorihui@scut.edu.cn)

This work was supported in part by MOST, in part by the Guangdong Natural Science Foundation under Grant 2016A030313459 and Grant 2017A030310028, in part by the Guangdong Science and Technology Project under Grant 2016B090907001, Grant 2016A040403037, Grant 2016B090906002, and Grant 2017A050503002, in part by the Guangzhou Science and Technology Project under Grant 201804020033, and in part by the Project for Guangdong Province Universities and Colleges Pearl River Scholar Funded Scheme (2016).

ABSTRACT Solution-processed oxide dielectrics are widely studied as alternatives to SiO_2, SiN_x in thin film transistors for high capacitance and low energy consuming. However, it's still a challenge to achieve high quality of solution-processed oxide dielectrics TFT by low-temperature post-treatment. Here, an effective strategy is proposed to evaluate low temperature solution-processed ZrO_2 TFT in terms of uniformity, film density and electrical performance by employing TG/DSC, drop analyzer, XRR and a novel μ-PCD measurement. Particularly, μ-PCD measurement provides valuable information on homogeneity and defect level. The optimized device with $ZrNO_3$ as dielectric precursor and ethyl alcohol as solvent through spin coating process annealed at 200°C shows a saturation mobility of 8.6 $cm^2V^{-1}S^{-1}$, I_{on}/I_{off} ratio about 1.1×10^6, subthreshold swing about 334 mV/decade with a low leakage current density of 5×10^{-5} A/cm^2 at 10V. This article offers a convenient way for precursor optimization towards low leakage current and high homogeneity solution-processed oxide dielectrics for TFT devices.

INDEX TERMS TFT, solution-processed, oxide dielectric, microwave photoconductivity decay, subthreshold swing (SS).

I. INTRODUCTION

Metal oxide dielectrics have recently emerged as promising alternatives to SiO_2, SiN_x in thin film transistors (TFTs) owing to their superior properties, including high capacitance, low defect states and large band gap which leads to high mobility and low off-current [1]–[3]. For these reasons, oxide dielectrics fabricated by vacuum process are widely studied in displays, sensor arrays, and driving circuits. Meanwhile, solution process has also received remarkable attention because of the advantage of low-cost for large scale fabrication including spin coating, inkjet printing, spray-coating, and slit coating [4]–[7]. However, high temperature annealing process limits the application in flexible display. Compared to ALD method and combustion synthesis which can achieve high quality film at low temperature, solution engineering method or UV fast curing process have the advantage of convenience and practicality in large scale fabrication [8], [9]. What' more, large leakage current and inhomogeneity for solution-processed oxide dielectrics still remain problems especially in flexible devices [10], [11].

The conventional way for evaluating dielectric film quality for solution-processed TFT device is from the output and transfer curves of various conditions, which is incomprehensive for optimization of precursor system [12], [13]. Measurement on precursor ink and fabricated film including

thermal gravimetric (TG)/differential scanning calorimetry (DSC), physical characteristics (viscosity and surface tension) and X-Ray Reflectometry (XRR) can provide valuable information.

What's more, it is hard to evaluate the homogeneity of dielectric film. Known as a non-destructive, non-contact and high-efficiency measurement, microwave photoconductivity decay (μ-PCD) method was widely used for process control and semiconductors evaluation [14]. Yasuno *et al.* have reported the uniformity judgement of In-Ga-Zn-O (IGZO) on glass substrate by the μ-PCD measurement [15]. Goto *et al.* implemented in-line process monitoring for the fabrication of a-IGZO TFTs using a microwave detected photoconductivity decay technique [16]. We introduce μ-PCD method to evaluate the homogeneity of dielectrics as well as defects between semiconductor/insulator interface by measuring IGZO film deposited on the top.

In this work, an effective evaluation strategy is proposed to prepare low temperature solution-processed oxide dielectric TFTs with good uniformity and low leakage current. As we know, zirconia (ZrO_2) is a widely used metal oxide insulator with high bad gap, high capacitance and low trap density, as well as good solution processability [17]. Five ZrO_2 solution was synthesized and evaluated. Film density, roughness and electrical performance were obtained and analyzed. In addition, homogeneity and defect level were evaluated by a novel micro-PCD method. The films and devices annealed at 200°C showed strong correlation between several measurement and electrical properties, providing an effective strategy for optimization of solution-processed oxide dielectrics.

II. EXPERIMENTAL PROCEDURE

In our experiment, Zirconium nitrate ($ZrNO_3$), zirconium acetate ($Zr(CH_3COO)_4$) and zirconium oxychloride ($ZrOCl_2$) were adopted as precursor. Precursor was dissolved in various good solvents for inorganic salt including ethyl alcohol (EtOH), ethylene glycol (EG) and deionized water (H_2O) to achieve high solubility, good dispersity solution. Solutions with $ZrNO_3$ as precursor and EtOH as solvent was denoted as Ink-1 ($ZrNO_3$+EtOH), other solution were denoted as Ink-2 ($ZrNO_3$+EG), Ink-3 ($ZrNO_3$+H_2O), Ink-4 ($Zr(CH_3COO)_4$+EtOH) and Ink-5 ($ZrOCl_2$+EtOH) respectively. The optimized concentration for all solution was 0.3M, as large as possible within the solubility of solvents. Then they were stirred at 500 r/min at room temperature for 2 hours and aged for 24h. Spin coating method was adopted to prepare large area dielectric films with speed of 5000rpm for 40s, annealed at 200°C under atmospheric environment for 1 hour. For μ-PCD test, same 50nm-thick direct current sputtered (DC-sputtered) IGZO was fabricated with power of 100W, pressure of 1mTorr (oxygen:argon=5%), pulse frequency of 10kHz and reverse time of 10μs on the top of various ZrO_2 films. Metal/insulator/metal (MIM) devices were prepared using a sandwich structure of ITO/ZrO_2/Al. ZrO_2-TFTs employed bottom gate top contact structure were fabricated by following steps: ZrO_2 films were coated on the ITO substrate, and 10nm-thick DC sputtered IGZO was deposited using the same method mentioned above; finally, Al source/drain electrodes with 150nm thick were deposited by sputtering at room temperature.

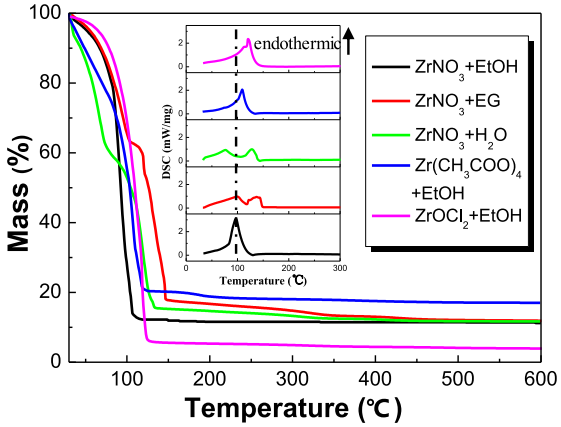

FIGURE 1. TG/DSC measurement of various inks.

The electrical properties of the ZrO_2 TFTs were tested by a semiconductor parameter analyzer (Agilent4155C, Agilent). Saturation mobility was extracted from the curve of $I_D^{1/2}$ versus the V_G in saturated operation region using eq (1), and the subthreshold swing (SS) was obtained from the inverse of the maximum slope of the curve of Log I_D versus the V_G using eq (2), where C_i is the capacitance per unit area of the gate insulator, I_D is the drain current, V_G is the gate voltage, and V_{th} is the threshold voltage, W and L are the channel width and length, respectively.

$$I_D^{1/2} = \left(\frac{WC_i\mu_{sat}}{2L}\right)^{1/2}(V_G - V_{th}) \quad (1)$$

$$SS = \left[\left(\frac{dLogI_D}{dV_G}\right)_{\max}\right]^{-1}. \quad (2)$$

III. RESULTS AND DISCUSSION

Figure 1 shows the TG/DSC test of different dielectric precursor. Test was performed from 30 to 600°C in alumina crucible with heating rate of 10K/min under nitrogen atmosphere by Netzsch STA 449C. Primary mass lost happened below 200°C for all samples and the products were less than 20% of total weight. Ink-1 revealed the lowest reaction temperature around 100°C, owing to the volatile nature of ethyl alcohol and the low hydrolysis temperature of $ZrNO_3$ [18]. DSC results were consistent with TG results. It is noteworthy that samples with EtOH as solvent including ink-1, ink-4 and ink-5 exhibited only one endothermic peak, but samples with H_2O or EG as solvent exhibited two peaks mainly because of large difference in volatilization and hydrolysis temperature for precursor and solvent. The removal of solvent and transformation into oxide film for the solution is related to the degree of endothermic reaction which can be revealed from value of endothermic peak. Obviously, the peak value for solution with EtOH as solvent

TABLE 1. Physical characteristics of various inks.

Property (20℃) / Solution	Solubility	Viscosity (mPa·s)	Surface tension (mN/m)
Ink-1 ($ZrNO_3$+EtOH)	Good	1.2	24.3
Ink-2 ($ZrNO_3$+EG)	Good	2.3	48.6
Ink-3 ($ZrNO_3$+H_2O)	Good	1.1	72.0
Ink-4 ($Zr(CH_3COO)_4$+EtOH)	Common	1.9	25.6
Ink-5 ($ZrOCl_2$+EtOH)	Good	1.7	26.4

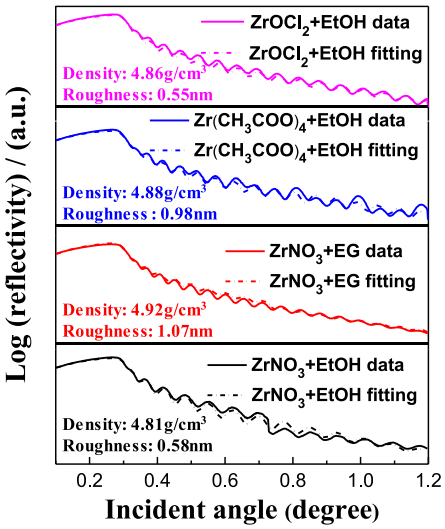

FIGURE 2. XRR measurement of dielectric films from various inks.

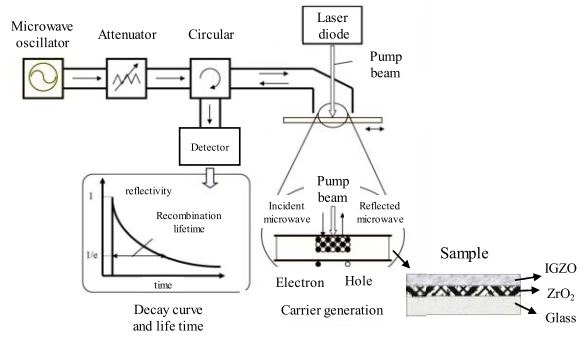

FIGURE 3. Principle of μ-PCD method.

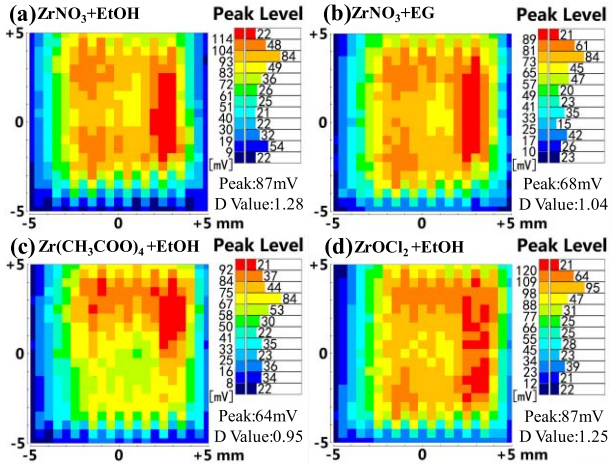

FIGURE 4. μ-PCD map scanning of peak value for sputtered IGZO on various dielectric films from (a) ink-1; (b)ink-2; (c) ink-4 and (d) ink-5 solution.

were larger than solution with H_2O or EG as solvent, confirming the reaction for solution with EtOH as solvent were more sufficient at low temperature. Both samples showed potential in low temperature annealing process especially for ink-1.

The physical characteristics of inks have a great influence on film formation process and the final electrical properties which is summarized in Table 1 [19], [20]. The viscosity and surface tension of inks was measured by HAAKE MARS 40 and Attention (Biolin Scientific). The solubility for ink-4 was worse than other inks, which could lead to non-uniform film formation during coating process as it will introduce impurities. What's more, ink-3 failed to achieve integrated films due to overlarge surface tension (72mN/m). It is worth mentioning that for other solution process the demand for viscosity and tension might be different.

Density and roughness of films fabricated were obtained by fitting the interference fringe of X-ray using EMPYREAN in Figure 2 [21]. No significant difference was found in the density of all samples (4.81-4.92g/cm^3). Roughness for films from ink-1 and ink-5 was as low as around 0.5nm while that for ink-2 and ink-4 was around 1nm. The XRR results indicated solubility and surface tension play important parts in surface roughness of films for spin coating process [22].

In order to estimate the film uniformity and interface defect between semiconductor and gate insulator, microwave photoconductivity decay (KOBELCO) with microwave oscillator of 9.6GHz and laser wavelength of 349nm was employed in atmospheric environment, which is demonstrated in Figure 3. The scanning area was 0.5∗0.5mm each point. The quality of IGZO films were evaluated by a decay curve which obtained characterization of the capture, recombination, and relaxation of photo-generated carriers [23]. Since dielectric films have significant influence on the adjacent semiconductor layer, the quality of ZrO_2 films could be estimated by the measurement on semiconductor fabricated on the top of dielectric films [24]. Two critical parameters were obtained from the μ-PCD test. The Peak value, which originates from the recombination processes of photo-generated carriers during laser pulse irradiation, is related to the density of the conduction band tail states. And D value is attributed to the density of the sub gap states which is related with trapping processes by defects. High Peak value and D value represents film of high quality and good interface contact [14].

Figure 4 represents μ-PCD map scanning of peak value for various samples. Samples from ink-1 and ink-5 exhibited highest peak value of 87mV and approximate D value.

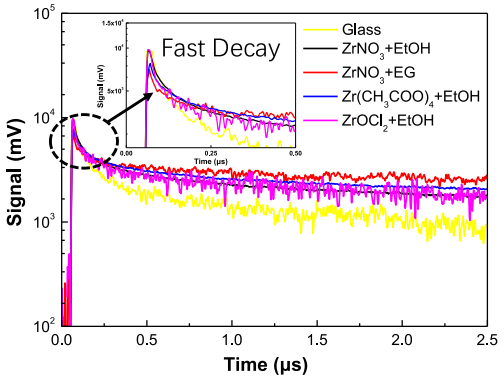

FIGURE 5. Obtained decay curve by μ-PCD of different samples.

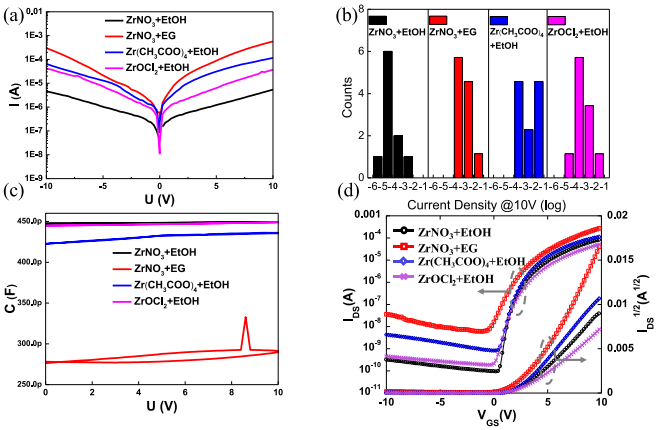

FIGURE 6. (a) Leakage current density of spin-coated dielectrics; (b) histograms of leakage current density distribution; (c) C-V curve and (d) transfer characteristic of IGZO TFTs with different dielectrics.

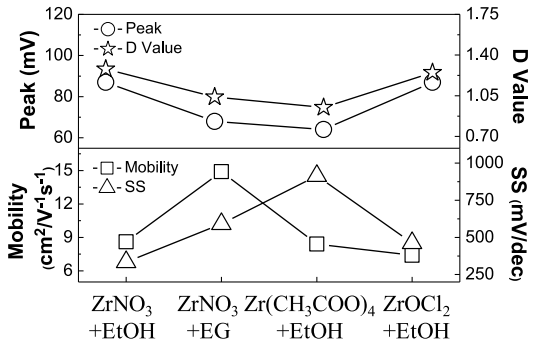

FIGURE 7. Tendency of mobility, subthreshold swing, peak value and D value.

IGZO on films from ink-2 and ink-4 showed deteriorative peak value and D value probably because of high surface tension of ethylene glycol and poor solubility of $Zr(CH_3COO)_4$ precursor which resulted in porous ZrO_2 films with large amount of interface defect, making it impossible to generate sufficient carriers. In addition, circular distribution of peak value for a $10 * 10$mm size sample were observed owing to spin coating process except for sample from ink-4, confirming that solubility plays a crucial role in the homogeneity of spin coating oxide films.

Figure 5 is obtained decay curve by μ-PCD method [25]. The built-in figure exhibits the enlarged view of fast decay period of the decay process. IGZO on dielectric film from ink-1 and ink-5 showed higher peak signal of more than 9000 mV while that for samples from ink-2 and ink-4 was around 6500mV. This indicates samples with dielectrics from ink-1 and ink-5 were of better quality. What's more, the attenuation for IGZO was sufficient for samples from ink-1 and ink-5 as it decayed to 1000mV after 2.5μs, while samples from ink-2 exhibited worse result with around 3000mV, corresponding to the long lifetime of photogenerated carriers caused by defects at the interface [26]. Decay curves provided valuable information on interface contact of IGZO/ZrO_2.

Figure 6 (a) represents leakage current density of dielectrics annealed at 200°C. The thickness for all samples was similar (62-73nm). Dielectric from ink-1 exhibited lowest leakage current density ($5 * 10^{-5}$A/cm^2 at 10V). Figure 6 (b) shows histograms of leakage current density distribution of each sample. Apparently, leakage current density followed Gaussian distribution except for ink-4 sample. This was consistent with μ-PCD map scanning results that poor solubility resulted in non-uniform film formation process. Figure 6 (c) exhibits C-V curves of dielectrics from various solution. Obviously with similar thickness the capacitance should be close for each sample. Sample from ink-1 and ink-5 showed almost the same capacitance of 450nF and scarcely changed with increasing voltage. Sample from ink-2 showed lower capacitance of 430nF probably because of the impurities in the film. Sample from ink-4 exhibited much lower capacitance and a large hysteresis during sweeping forth and back. This could be ascribed to the residual organic solvent and large number of defects existed in the film. Figure 6 (d) is the transfer characteristic of IGZO TFTs. TFTs with dielectric film from ink-1 had largest I_{on}/I_{off} ratio owing to lowest leakage current. Unexpectedly TFT with dielectric from ink-2 achieved highest mobility of 14.9cm^2/(V·s) even with large leakage current. High mobility of this device might be derived from large leakage current especially at on state.

In Figure 7 the tendency of peak and D value results went exactly against with SS. Small SS value indicates lower trap density of in the channel layer or interface [27], [28]. Devices with dielectrics from ink-1 and ink-5 solution obtained smallest SS value of less than 500mV/dec and largest peak value of 85∼87mV as well as D value of 1.25∼1.28. Strong connections between obtained results and transistor performance were founded. In summary, device with dielectric from ink-1 exhibited best electrical performance and excellent uniformity, with leakage current density of 5×10^{-5}A/cm^2, saturation mobility of 8.6cm^2/V^{-1}s^{-1}, I_{on}/I_{off} ratio of 1.1×10^6 and SS of 334mV/dec.

IV. CONCLUSION

In conclusion, an effective evaluation strategy towards low temperature solution-processed ZrO_2 dielectric TFTs is proposed [29]. As a result, strong correlation between several measurement and electrical properties were found. TG/DSC test indicated lowest film-forming temperature and XRR results proved that dense structure was formed for ink-1 (solution of $ZrNO_3$ as precursor and EtOH as solvent). Meanwhile, film from ink-1 showed highest Peak and D value in μ-PCD measurement, indicating good electrical property and few interface defects, proved by leakage current density test and transfer characteristic curves. The nondestructive μ-PCD method along with other measurement for solvent and film offer a convenient and effective way for precursor evaluation and optimization of solution-processed oxide dielectrics for TFT devices.

REFERENCES

[1] E. Fortunato, P. Barquinha, and R. Martins, "Oxide semiconductor thin-film transistors: A review of recent advances," *Adv. Mater.*, vol. 24, pp. 2945–2986, May 2012.

[2] T. Kamiya and H. Hosono, "Material characteristics and applications of transparent amorphous oxide semiconductors," *NPG Asia Mater.*, vol. 2, pp. 15–22, Jan. 2010.

[3] J. S. Park, W.-J. Maeng, H.-S. Kim, and J.-S. Park, "Review of recent developments in amorphous oxide semiconductor thin-film transistor devices," *Thin Solid Films.*, vol. 520, no. 6, pp. 1679–1693, 2012.

[4] S. J. Kim, S. Yoon, and H. J. Kim, "Review of solution-processed oxide thin-film transistors," *Jpn. J. Appl. Phys.*, vol. 53, no. 2, Jan. 2014, Art no. 02BA02.

[5] S. Park, C.-H. Kim, W.-J. Lee, S. Sung, and M.-H. Yoon, "Sol-gel metal oxide dielectrics for all-solution-processed electronics," *Mater. Sci. Eng. R Rep.*, vol. 114, pp. 1–22, Apr. 2017.

[6] W. Xu, H. Wang, L. Ye, and J. Xu, "The role of solution-processed high-K gate dielectrics in electrical performance of oxide thin-film transistors," *J. Mater. Chem. C.*, vol. 2, no. 27, pp. 5389–5396, 2014.

[7] J.-Y. Kwon, D.-J. Lee, and K.-B. Kim, "Review paper: Transparent amorphous oxide semiconductor thin film transistor," *Electron. Mater. Lett.*, vol. 7, no. 1, pp. 1–11, 2011.

[8] J. Yang, B. Wang, Y. Zhang, X. Ding, and J. Zhang, "Low-temperature combustion synthesis and UV treatment processed p-type Li: NiOx active semiconductors for high-performance electronics," *J. Mater. Chem. C.*, vol. 6, no. 46, pp. 12584–12591, 2018.

[9] X. Ding, J. Yang, C. Qin, X. Yang, T. Ding, and J. Zhang, "Nitrogen-doped ZnO film fabricated via rapid low-temperature atomic layer deposition for high-performance ZnON transistors," *IEEE Trans. Electron Devices*, vol. 65, no. 8, pp. 3283–3290, Aug. 2018.

[10] J. Socratous *et al.*, "Electronic structure of low-temperature solution-processed amorphous metal oxide semiconductors for thin-film transistor applications," *Adv. Funct. Mater.*, vol. 25, no. 12, pp. 1873–1885, 2015.

[11] S.-Y. Liu, J. Pan, J.-G. Lu, and H.-P. D. Shieh, "A pressure-sensitive impedance-type touch panel with high sensitivity and water-resistance," *IEEE Electron Device Lett.*, vol. 39, no. 7, pp. 1061–1064, Jul. 2018.

[12] S. W. Cho *et al.*, "Chemical durability engineering of solution-processed oxide thin films and its application in chemically-robust patterned oxide thin-film transistors," *J. Mater. Chem. C.*, vol. 5, no. 2, pp. 339–349, 2017.

[13] L. Xifeng, X. Enlong, and Z. Jianhua, "Low-temperature solution-processed zirconium oxide gate insulators for thin-film transistors," *IEEE Trans. Electron Devices*, vol. 60, no. 10, pp. 3413–3416, Oct. 2013.

[14] S. Yasuno, T. Kugimiya, S. Morita, A. Miki, F. Ojima, and S. Sumie, "Correlation of photoconductivity response of amorphous In-Ga-Zn-O films with transistor performance using microwave photoconductivity decay method," *Appl. Phys. Lett.*, vol. 98, no. 10, Mar. 2011, Art. no. 102107.

[15] S. Yasuno, T. Kita, S. Morita, T. Kugimiya, K. Hayashi, and S. Sumie, "Transient photoconductivity responses in amorphous In-Ga-Zn-O films," *J. Appl. Phys.*, vol. 112, no. 5, 2012, Art. no. 053715.

[16] H. Goto *et al.*, "In-line process monitoring for amorphous oxide semiconductor TFT fabrication using microwave-detected photoconductivity decay technique," *IEICE Trans. Electron.*, vol. E97.C, no. 11, pp. 1055–1062, 2014.

[17] K. Yim *et al.*, "Novel high-K dielectrics for next-generation electronic devices screened by automated AB initio calculations," *NPG Asia Mater.*, vol. 7, no. 6, 2015, Art. no. e190.

[18] H. Wang *et al.*, "Solvent effects on polymer sorting of carbon nanotubes with applications in printed electronics," *Small*, vol. 11, no. 1, pp. 126–133, 2015.

[19] P. N. Plassmeyer, G. Mitchson, K. N. Woods, D. C. Johnson, and C. J. Page, "Impact of relative humidity during spin-deposition of metal oxide thin films from aqueous solution precursors," *Chem. Mater.*, vol. 29, no. 7, pp. 2921–2926, 2017.

[20] J. H. Park *et al.*, "Boron-doped peroxo-zirconium oxide dielectric for high-performance, low-temperature, solution-processed indium oxide thin-film transistor," *ACS Appl. Mater. Inter.*, vol. 5, no. 16, pp. 8067–8075, 2013.

[21] H.-Y. Park, A. Song, D. Choi, H.-J. Kim, J.-Y. Kwon, and K.-B. Chung, "Enhancement of the device performance and the stability with a homojunction-structured tungsten indium zinc oxide thin film transistor," *Sci. Rep.*, vol. 7, no. 1, 2017, Art. no. 11634.

[22] W. He *et al.*, "Surface modification on solution processable zro_2 high-k dielectrics for low voltage operations of organic thin film transistors," *J. Phys. Chem. C.*, vol. 120, no. 18, pp. 9949–9957, 2016.

[23] J. Chen *et al.*, "Evaluation of Nd-Al doped indium-zinc oxide thin-film transistors by a μ-PCD method," *Semicond. Sci. Technol.*, vol. 34, no. 5, 2019, Art. no. 55011.

[24] A. Zeumault and V. Subramanian, "Mobility enhancement in solution-processed transparent conductive oxide TFTs due to electron donation from traps in high-k gate dielectrics," *Adv. Funct. Mater.*, vol. 26, no. 6, pp. 955–963, 2016.

[25] X. Liu *et al.*, "A novel nondestructive testing method for amorphous Si-Sn-O films," *J. Phys. D Appl. Phys.*, vol. 49, no. 50, 2016, Art. no. 505102.

[26] H. Im *et al.*, "Accurate defect density-of-state extraction based on back-channel surface potential measurement for solution-processed metal-oxide thin-film transistors," *IEEE Trans. Electron Devices.*, vol. 64, no. 4, pp. 1683–1688, Apr. 2017.

[27] L.-Y. Su, H.-Y. Lin, H.-K. Lin, S.-L. Wang, L.-H. Peng, and J. Huang, "Characterizations of amorphous IGZO thin-film transistors with low subthreshold swing," *IEEE Electron Device Lett.*, vol. 32, no. 9, pp. 1245–1247, Sep. 2011.

[28] W. Cai *et al.*, "Investigation of direct inkjet-printed versus spin-coated ZrO_2 for sputter IGZO thin film transistor," *Nanoscale Res. Lett.*, vol. 14, no. 1, 2019, Art. no. 80.

[29] Y. M. Park, A. Desai, A. Salleo, and L. Jimison, "Solution-processable zirconium oxide gate dielectrics for flexible organic field effect transistors operated at low voltages," *Chem. Mater.*, vol. 25, no. 13, pp. 2571–2579, 2013.